

Influence of Tire Footprint Area and Pressure Distribution on Pavement Responses

Fabricio Leiva-Villacorta, Adriana Vargas-Nordbeck,
José P. Aguiar-Moya and Luis Loria-Salazar

Abstract For most pavement analyses, it is assumed that the tire load is uniformly applied over a circular area. Also, it is generally assumed that tire inflation and contact pressures are uniform throughout the contact area. Several studies on this topic have shown different non-uniform pressure patterns. Therefore, a full understanding of the interaction between tires and pavement is necessary to obtain more accurate pavement responses. The objective of this study was to evaluate the effects of truck tire contact pressure on pavement responses at different loading conditions. A tire footprint system was used to capture contact pressure patterns statically and dynamically (low speed) at three inflation pressures and three wheel loads. All testing conditions were performed using a Heavy Vehicle Simulator HVS Mark VI with a five-rib tire type 11R22-5. A flexible pavement section instrumented with asphalt strain gauges, pressure cells and multi depth deflectometers was used to measure pavement responses. Measured tire-pavement contact stress data were input into a finite element analysis program to compute pavement responses and compare them to the measured responses. The contact pressure patterns obtained for the five-rib tire indicated that higher pressures were obtained for the inner ribs based on the controlled variables. In general, the results indicated that the contact area decreased for a given load as the inflation pressure was increased. Statistical analysis confirmed that pavement responses were significantly related to tire pressure distribution.

F. Leiva-Villacorta (✉) · A. Vargas-Nordbeck · J.P. Aguiar-Moya · L. Loria-Salazar
LanammeUCR, San José 11501-2060, Costa Rica
e-mail: fabricio.leiva@ucr.ac.cr

A. Vargas-Nordbeck
e-mail: adriana.vargasnordbeck@ucr.ac.cr

J.P. Aguiar-Moya
e-mail: jose.aguiar@ucr.ac.cr

L. Loria-Salazar
e-mail: luis.loriasalazar@ucr.ac.cr

1 Introduction

The contact footprint patterns of a vehicle tire on a pavement structure and its corresponding pressure distribution related to the vehicle load variation may indicate the tire quality and the state of the tire wear and tear. Accordingly, measurement of a tire's contact footprint pattern and pressure distribution is useful in determining stress concentrations and determining possible causes of typical pavement distresses.

Pavement responses are closely related to long term pavement performance and distress. Fatigue cracking and rutting, two major flexible pavements distresses, could be related to immediate pavement responses and could be explained in a mechanistic way. Horizontal tensile strains at the bottom of the asphalt concrete layer can explain fatigue cracks that initiate at the bottom and progress to the pavement surface. In contrast, pavement cracks can also start at the pavement surface due to excessive tensile strains and progress downward (NCHRP 2004a, b; El-Basyouny 2004). Similarly, vertical compressive strains at the top of the subgrade are considered closely related to pavement rutting due to compaction and/or consolidation of the soil (Huang 1993).

The tire-pavement contact pressure distribution is significantly affected by tire inflation pressure, tire type, tire load and tire tread patterns. Many measuring systems have been developed to measure the tire-pavement contact pressure in the last decade. The measured data clearly reveal that the tire-pavement contact pressure distribution is non-circular, non-uniform and discontinuous (Roque et al. 2000; Beer et al. 1999).

Pavement responses can be measured directly using in situ instruments embedded in pavement structures. Over the past two decades, computer controlled instrumentation technology has been used to acquire real-time measurements of pavement responses to dynamic traffic loading. Mateos and Snyder (2002) tested four sections at the Minnesota Road Research facility (Mn/ROAD) with a moving load configured at various axle loadings and tire pressures and found that changes in tire pressure did not significantly affect pavement behavior. Al-Qadi et al. (2002) found that wide-base "super singles" were not more damaging to the Virginia Smart Road sections than dual tires and they also reported that the radial tires reduced strain at the bottom of the asphalt layer. Sebaaly and Tabatabaee (1992) found increased pavement stresses caused by high tire pressure tires and the wide-base "super singles", but they found the effect of high tire pressure was insignificant to pavement performance. Akram et al. (1993) from the Texas Transportation Institute (TTI) tested two thin and thick road sections with varying tire pressures and vehicle speeds and found that high tire pressures caused higher tensile strain at the bottom of the AC layer but had no significant effect on vertical strain at the top of subgrade.

Although measurement of pavement responses in a road test can provide the most direct real-time data, road tests are always expensive. Fortunately, aside from real pavement on-site measurements, a theoretical analysis method can also be employed to simulate pavement responses due to traffic loading. Two categories of analytical programs have been used in flexible pavement analysis, the elastic

multilayer model and the finite element model. Machemehl et al. (2005) and Prozzi and Luo (2005) used a multilayer program to compute asphalt pavement responses due to measured non-uniform tire-pavement contact stress and found tire pressure has significant effects on tensile strains at the bottom of the asphalt concrete layer, but the effect of tire pressure on vertical strains at the top of the subgrade is insignificant. Weissman (1999) used an elastic multilayer based program and non-uniform contact pressure distribution to predict the distress patterns of a pavement undergoing overloads at an accelerated loading facility. Siddharthan et al. (2002) computed pavement responses using a measured non-uniform contact stress as well as a uniform contact stress distribution and found the uniform method overestimated pavement responses. Wang and Machemehl (2006) used a finite element program to compute asphalt pavement responses due to measured non-uniform tire-pavement contact stress and found increased truck tire pressure can cause increased pavement distress for both cracking and rutting.

For most pavement analyses, it is assumed that the tire load is uniformly applied over a circular area. Also, it is generally assumed that tire inflation and contact pressures are uniform throughout the contact area. However, several of the studies mentioned above on this topic have shown different non-uniform pressure patterns. Therefore, a full understanding of the interaction between tires and pavement is necessary to obtain more accurate pavement responses.

1.1 Objective

The objective of this study was to evaluate the effects of truck tire contact pressure on pavement responses at different loading conditions at the full scale accelerated pavement facility of the University of Costa Rica—PaveLab.

In order to achieve this objective, a tire footprint system was used to capture contact pressure patterns statically and dynamically (low speed) at three inflation pressures and three wheel loads. All testing conditions were performed using a Heavy Vehicle Simulator HVS Mark VI with a five-rib tire type 11R22-5. A flexible pavement section instrumented with asphalt strain gauges, pressure cells and multi depth deflectometers was used to measure pavement responses. Measured tire-pavement contact stress data were input into a finite element analysis program to compute pavement responses and compare them to the measured responses.

1.2 Test Section

Table 1 shows the characteristics of the evaluated section with its respective layer thicknesses obtained from ground penetrating radar (GPR) measurements and backcalculated layer moduli based on Falling Weight Deflectometer results (FWD). These are the layer moduli computed when the pavement structure was intact.

Table 1 Test Track in-place properties

Properties\section	AC3
Asphalt concrete thickness (H1), cm	13.2
Base thickness (H2), cm	31.0
Subbase thickness (H3), cm	30.1
AC modulus (E1) @ 25 °C, MPa	3800
Granular base modulus (E2), MPa	170
Subbase modulus (E3), MPa	140
Subgrade modulus (E4), MPa	70

The top layer consists of an asphalt concrete (AC) mixture with nominal maximum aggregate size of 19.0 mm with an optimum binder content of 4.9 % by total weight of mixture. The cement treated base (CTB) was designed to withstand a compressive stress of 35 kg/cm² with an optimum cement content of 1.7 % by volume of aggregate and with a maximum density of 2013 kg/m³. The base material and granular sub-base were placed at a maximum density of 2217 kg/m³ with an optimum moisture content of 8.6 %. The sub-base material had a CBR of 95 %. Finally, the subgrade material was constructed for a maximum density of 1056 kg/m³ with an optimum moisture content of 52 % and CBR of 6.6 %.

1.3 Instrumentation

The experiment included not only the instrumentation integrated with the HVS system but also embedded instrumentation. HVS onboard sensors can record the applied load, tire pressure and temperature, position and velocity of the load carriage. Embedded instrumentation include asphalt strain gauges (PAST model H-shaped sensors), pressure cells (SOPT model transducer for soils), multi depth deflectometers (MDDs), moisture and temperature probes. These sensors were chosen based on previous HVS owner's experience (HVS 2015; Baker Harris et al. 1994). Additionally, the HVS was equipped with a laser profiler that can be used to create a three-dimensional profile of the section and a Road Surface Deflectometer (RSD) is added to the testing equipment to obtain deflection basins at any location along the test section (Leiva-Villacorta et al. 2013, 2015).

Figure 1 shows the instrumentation array used for the experimental section. The PAST sensors were placed at the base/HMA layer interface in the longitudinal or traffic loading direction and in the transverse direction. MDD sensors were installed at 4 different depths to cover all four structural layers. The thermocouples were placed at four depths: surface, middle depth of the AC layer, at the PAST sensors depth and 5 cm into the base layer.

Data collection of the 3D profile, strain, pressure, temperature and deflection is performed based on load repetitions. At the beginning of the test, data is obtained at short intervals. After 20,000 load repetitions, data is collected on a daily basis. Inspection of fatigue and reflective cracking, friction loss, loss of aggregate-asphalt

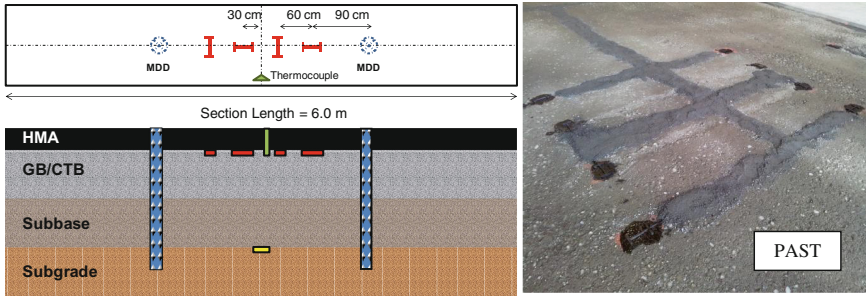


Fig. 1 Sensor array

bond and any other surface damage is performed on a daily basis during the HVS daily maintenance work.

1.4 Tire Footprint Acquisition System

A large high-resolution sensor, compatible with a wide range of tire sizes was used to capture tire footprint pressure patterns. Tire footprints can be captured statically or dynamically and are displayed as high resolution, multi-colored images of the tire contact pressure pattern in real time. The system’s application specific graphing and image analysis software enables quantitative and qualitative analysis of the tire footprint. Figure 2 exhibits the pressure sensor, the sensor handle which is used to transmit the sensor data to the Wireless/Datalogger Unit and a picture of the sensor being used with the tire load configuration of Heavy Vehicle Simulator (HVS) Mark VI. The software displays the pressure distribution data in multiple formats and the user has the option to create and customize graphs from the corresponding “movie” data or export as an ASCII file for use with other programs.



Fig. 2 Tire footprint acquisition system

The sensor consists of a square matrix of 425 mm with a thickness of 0.381 mm and 1936 pressure sensing elements (sensors). The maximum recordable pressure is 3447 kPa (500 psi). An equilibration device is used for improving accuracy and lifespan of the sensor. During equilibration, the sensor is inserted between a flat backing plate and an air filled bladder, which is inflated in order to apply a uniform pressure to the active area of the sensor. The equilibration process allows the software to compensate for any variation or uneven output across individual sensing elements caused by manufacturing or repeated use of the sensor. Equilibration devices are useful to perform quality assurance checks on the sensor and confirm uniform output by the sensor.

The tire footprint acquisition system is a resistive-based technology. The application of a normal force to an active sensor results in changes in the resistance of each sensing element (sensing element) in inverse proportion to the force applied. A multi-point calibration procedure was performed at a range closed to the expected tire pressure from 344 to 1379 kPa (50–200 psi).

2 Pressure Measurement

The tire-pavement contact pressure data were measured on a 11R22-5 tire which is part of the dual load configuration of the Heavy Vehicle Simulator Mark VI. This tire type was tested for nine load-inflation combinations: three tire loads and three inflation pressures. The 11R22-5 tire was chosen because its size is among the most typical in Costa Rica (Sibaja 2014). Figure 3 shows two examples of the tire footprint and vertical pressure distribution for different loads and pressures. The five tire treads or ribs are clearly defined and for all the cases evaluated in this study the center tread had higher pressures.

The pressure data can be exported to any type of spreadsheet such that the results can be analyzed. Figure 4 exhibits an example of the analyzed data. It was determined that the pressure distribution along the majority of the tire treads can be

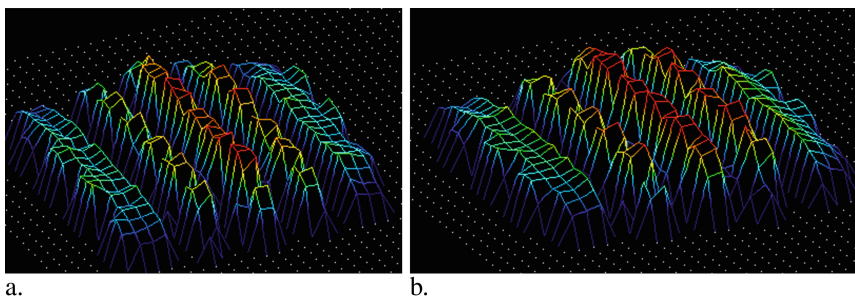


Fig. 3 Tire footprint and pressure distribution. **a** 40 kN and 586 kPa and **b** 50 kN and 689 kPa

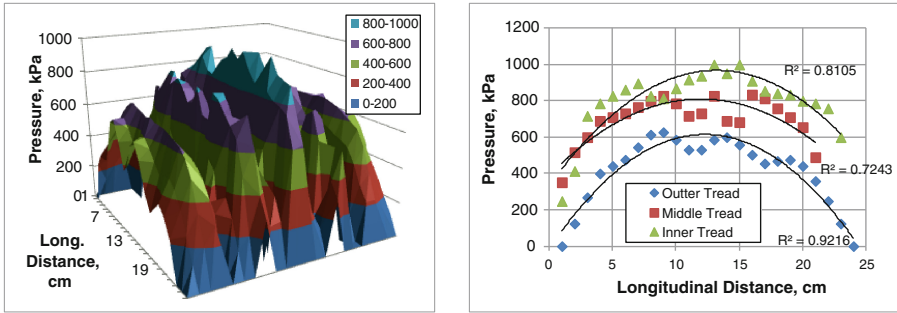


Fig. 4 Example of exported and evaluated pressure data

approximated with a parabolic function. On the other hand, further analysis was performed to quantify the change in the footprint. Table 2 shows the change in the maximum length of the wheel path (footprint), the maximum width and contact area for all 9 load-inflation combinations. As expected the maximum length was located in the center tread and tended to decrease as the load or pressure increases. For all cases the maximum width remained the same at 22.1 cm. On the other hand, the contact area determined by the number of sensing elements (sensels) was determined for static and dynamic loading (speed of 2 km/h). For static loading the contact area tended to increase as the load or pressure was increased while the opposite behavior, but to a lesser degree, was observed for dynamic loading. Finally, the peak contact pressure was significantly higher for static loading and tended to increase as the load or pressure was increased. The same trend, but in a less significant degree, was observed for peak pressures under dynamic loading.

Table 2 Measured wheel path properties

Load (kN)	Pressure (kPa)	Wheel max. length (cm)	Contact area (cm ²)	Peak pressure (kPa)
		Static/dynamic	Static/dynamic	Static/dynamic
40	586	23.1/22.5	292.7/233.4	1043/966
40	689	22.4/21.1	293.1/230.1	1296/1013
40	793	22.1/20.3	292.5/227.3	1537/1041
50	586	22.8/22.3	293.8/290.1	1050/960
50	689	23.8/21.6	303.6/285.1	1220/972
50	793	23.1/22.1	312.1/264.6	1516/1165
60	586	22.2/21.9	324.7/322.2	1099/961
60	689	25.4/25.1	335.3/317.6	1296/976
60	793	24.9/23.4	356.8/311.7	1434/1054

3 Modeled Pavement Responses

This part of the study involved prediction of pavement responses based on the actual footprint pressure distribution and a circular load with uniform distribution and then compare those results against measured tensile strain responses. In order to do this, it was necessary to determine the layer moduli at the moment when the tensile strains were obtained. Later, a finite element analysis software was used to set the tire treaded shape and apply the parabolic pressure distribution.

3.1 Backcalculated Layer Moduli

Multi-depth deflectometer (MDD) data were used to determine the progression of the pavement layer moduli. This was done by applying the method of equivalent thickness (Ullidtz 1987) whereby the thickness of the structure is transformed into a single layer. This transformation is done using Odemark’s methodology and calculation of stresses, strains and deflections were performed using Boussinesq’s theory.

Figure 5 shows an example of the backcalculated layer moduli for the different layers for one of the test tracks as function of equivalent load repetitions in millions. A good correlation was obtained between measured and estimated deflections and a small deviation from the line-of-equality indicated the criteria to perform back-calculation was sound and ensured that the methodology was successfully applied to each particular data set. When the tensile strains were obtained and the load-pressure was applied, the modulus of the asphalt concrete layer was estimated to be 1400 MPa, the modulus of the granular base and subbase were 125 MPa and the modulus of the subgrade was 50 MPa.

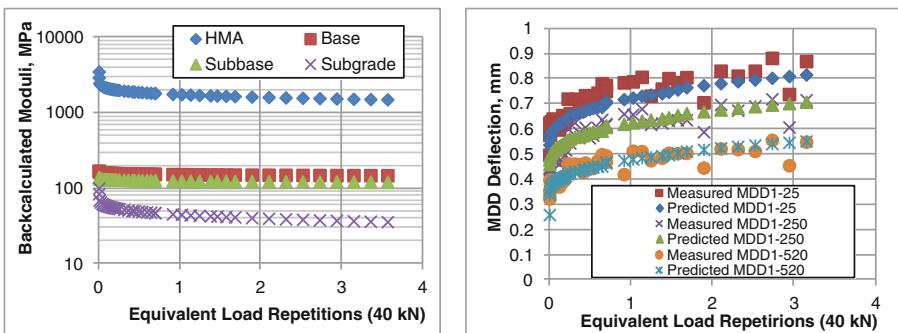


Fig. 5 MDD backcalculated layer moduli

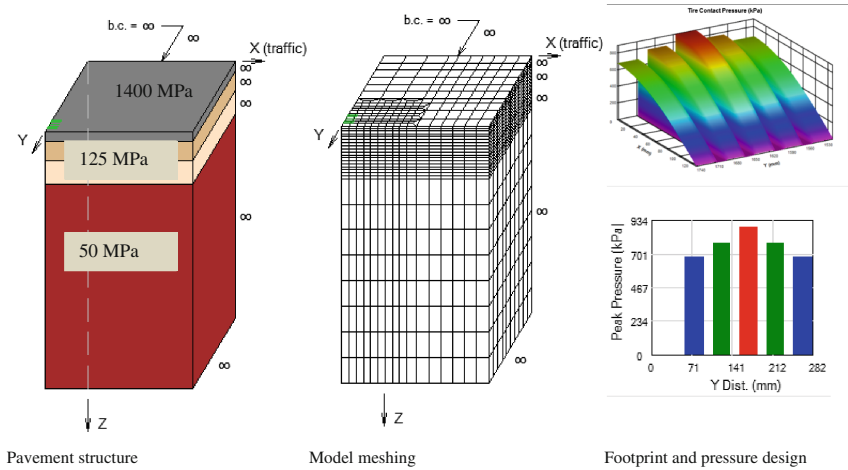


Fig. 6 Example of the evaluated structure

3.2 Load and Structure Modeling

A finite element analysis was used to model the tire treaded shape and to apply the parabolic pressure distribution. The three-dimensional (3D) finite-element based software package EverStressFE 1.0 was used for the analysis of the flexible pavement section subjected to the various wheel/axle load combinations. This software takes advantage of symmetry and utilizes a 1/4 pavement configuration. In this case, a dual tire load was simulated either with a parabolic approximation of the actual treaded load and a circular load to estimate pavement responses. An example of the modeled pavement structure, with the model meshing and the designed footprint and pressure distribution is given in Fig. 6. All the modeled load and pressure distribution for the treaded tire load were done under dynamic loading results because the actual responses were obtained under dynamic loading.

4 Measured Versus Predicted Strains

Figures 7 and 8 are examples of the measured and predicted longitudinal and transverse tensile strains obtained at the asphalt concrete/base interface. Measured strain signals exhibit a viscoelastic behavior with a significant difference in the shape of the signal (asymmetrical) when the wheel load approaches the sensor location and when it moves away from the sensor. In contrast, predicted strain responses based on layered elastic properties have a symmetrical behavior.

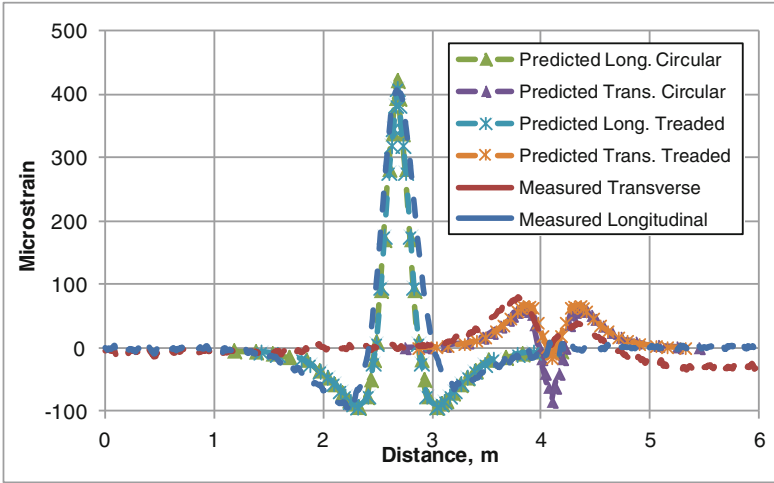


Fig. 7 Measured versus predicted tensile strains at 40 kN and 689 kPa

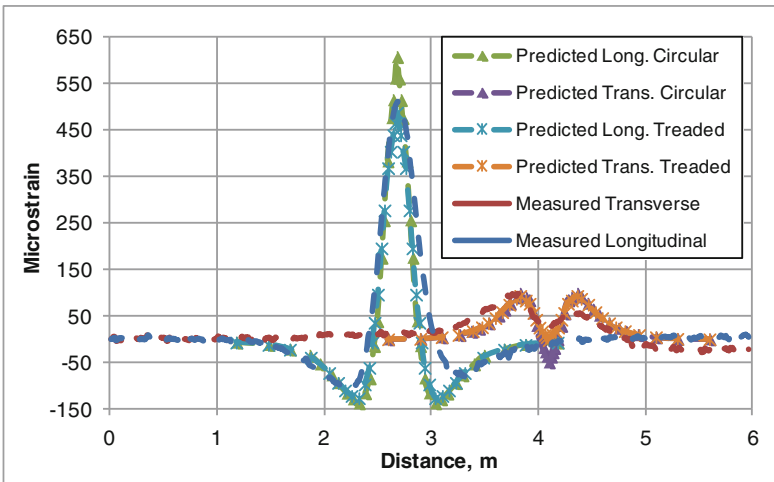


Fig. 8 Measured versus predicted tensile strains at 60 kN and 689 kPa

Nevertheless, predicted strain responses tended to reproduce fairly well the shape of the measured strain signal. Moreover, the treaded tire model exhibited a better match of the measured signal for both longitudinal and transverse strain. The circular load with uniform pressure distribution tended to overestimate the peak

longitudinal strain and tended to underestimate the minimum compressive strain of the transverse signal as shown in Figs. 7 and 8.

Figure 9 shows a comparison between measured and predicted responses. As mentioned above, the uniform circular load tended to overestimate the peak longitudinal tensile strain, specifically at high load-pressure combinations, while the non-uniform load provided a better agreement with actual peak values (closer to equality). On the other hand, both load configurations tended to underestimate the transverse peak tensile strain at low load-pressure combinations.

Another type of response measured in the field were deflections from MDD sensors. These deflections obtained at the surface of the pavement and 370 mm (bottom of the granular base) deep in the structure were also compared against predicted deflections. In this case both load configurations tended to match fairly well the actual deflections. Table 3 lists the critical horizontal strains at the bottom of the AC layer and deflections at two different depths of the pavement.

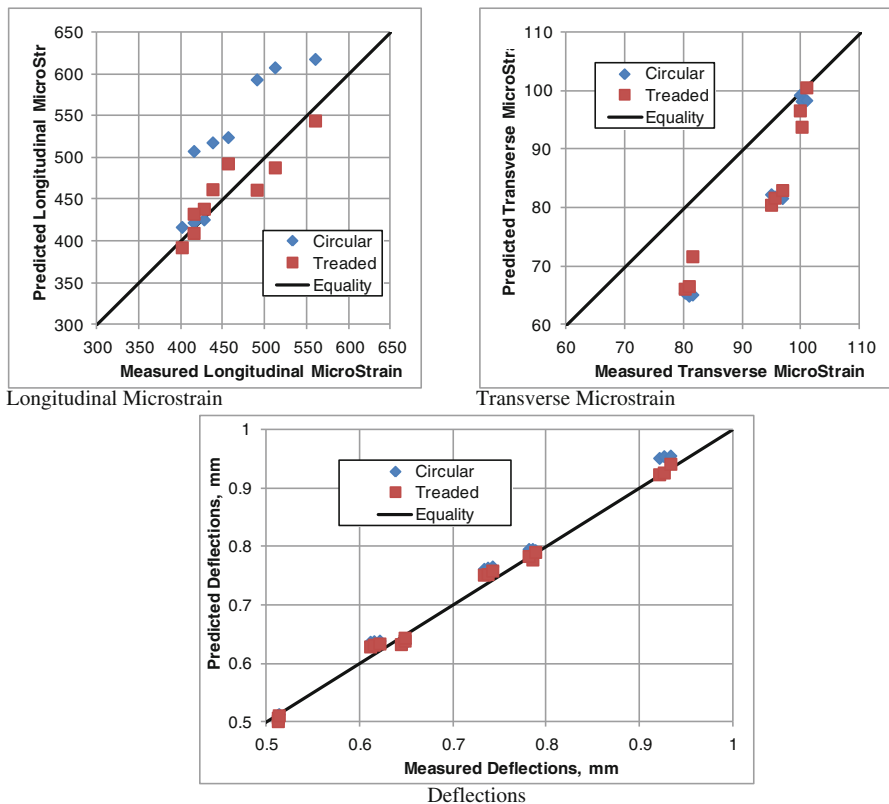


Fig. 9 Measured versus predicted responses

Table 3 Predicted and measured responses

Load (kN)	Pressure (kPa)	Load type	Modeled response			Measured response				
			ϵ_{long} ($\times 10^{-6}$)	ϵ_{trans} ($\times 10^{-6}$)	Surface deflection (mm)	Deflection @ 370 mm	ϵ_{long} ($\times 10^{-6}$)	ϵ_{trans} ($\times 10^{-6}$)	Surface deflection (mm)	Deflection @ 370 mm
40	586	Circular	416.8	65.42	0.636	0.511				
40	689	Circular	422.2	64.9	0.635	0.512				
40	793	Circular	425.8	65.1	0.634	0.513				
40	586	Treaded	392.4	66.1	0.633	0.507	401.3	80.2	0.644	0.512
40	689	Treaded	409.6	66.54	0.639	0.501	415.4	80.9	0.648	0.512
40	793	Treaded	438.6	71.66	0.644	0.511	427.6	81.5	0.648	0.513
50	586	Circular	507.9	82.28	0.796	0.637				
50	689	Circular	518.2	81.9	0.796	0.638				
50	793	Circular	524.5	81.63	0.794	0.639				
50	586	Treaded	432.6	80.48	0.778	0.629	415.5	94.9	0.785	0.611
50	689	Treaded	462.0	81.69	0.784	0.632	437.9	95.5	0.781	0.615
50	793	Treaded	493.0	83.01	0.791	0.634	456.3	96.8	0.788	0.621
60	586	Circular	593.7	99.31	0.952	0.762				
60	689	Circular	608.2	98.25	0.955	0.764				
60	793	Circular	618.3	98.4	0.956	0.766				
60	586	Treaded	461.4	96.65	0.924	0.752	490.6	99.8	0.921	0.733
60	689	Treaded	488.2	93.85	0.927	0.753	512.2	100.1	0.926	0.737
60	793	Treaded	544.4	100.6	0.942	0.759	560.1	100.9	0.933	0.742

5 Statistical Analysis

Tire inflation pressure (586, 689 and 793 kPa), tire load (40, 50 and 60 kN) and load type (circular and treaded) are the three loading parameters on which these tire-pavement contact stress predicted responses were based. All these parameters were analyzed and compared to study the effects of tire pressure on pavement responses. An analysis of variance (ANOVA) with a two way interaction model was used to compare sample means for all the different treatments and to evaluate their effects on pavement responses. Table 4 shows the test results for the effects of

Table 4 ANOVA of predicted responses

Response	Source	<i>df</i>	SS	MS	<i>F</i>	<i>p</i>
Long. strain	Load	2	54,602.7	27,301.4	1161.16	<0.5
	Pressure	2	4821.5	2410.8	102.53	<0.5
	Type	1	14,643.3	14,643.3	622.8	<0.5
	Load × type	2	7616.9	3808.4	161.98	<0.5
	Pressure × type	2	1697.4	848.7	36.1	0.003
	Error	4	94	23.5		
	Total	17				
	S	4.8489	R ²	99.89 %	R ² (adj)	99.52 %
Trans. strain	Load	2	2925.33	1462.66	1527.59	<0.5
	Pressure	2	16.06	8.03	8.38	0.037
	Type	1	0.64	0.64	0.67	0.46
	Load × type	2	16.51	8.25	8.62	0.035
	Pressure × type	2	20.35	10.17	10.63	0.025
	Error	4	3.83	0.96		
	Total	17				
	S	0.9785	R ²	99.87 %	R ² (adj)	99.46 %
Surface deflection	Load	2	0.280602	0.140301	53166.72	<0.5
	Pressure	2	0.000149	0.000074	28.19	0.004
	Type	1	0.00047	0.00047	178.19	<0.5
	Load × type	2	0.000548	0.000274	103.85	<0.5
	Pressure × type	2	0.000154	0.000077	29.2	0.004
	Error	4	0.000011	0.000003		
	Total	17				
	S	0.00177	R ²	99.99 %	R ² (adj)	99.97 %
Deflection @ 370 mm	Load	2	0.187751	0.093876	19997.2	<0.5
	Pressure	2	0.000059	0.00003	6.3	0.014
	Type	1	0.000228	0.000228	48.47	<0.5
	Error	12	0.000056	0.000005		
	Total	17				
	S	0.002166	R ²	99.97 %	R ² (adj)	99.96 %

all treatments on the horizontal tensile strains at the bottom of the AC layer and the two deflection responses.

The results indicated that the variability observed for the predicted longitudinal tensile strain, the transverse tensile strain and the surface deflection can be explained by the statistical difference of load level, pressure, the type of load and the interaction between type of load and load and pressure at a confidence level of 95 %. On the other hand, the variability of the predicted deflection at 370 mm deep into the structure can be explained by the statistical difference of the three main treatments at a confidence level of 95 %.

As expected, the tire load level is the main variable that can be used to explain the differences in all the analyzed pavement responses. In second order, the load type which is basically a comparison between uniform and non-uniform pressure distribution. This variable did not affect significantly the transverse peak tensile strain.

6 Conclusions

The following conclusions were based on the results of this study:

- In general, the results indicated that the contact area for dynamic loading decreased for a given load as the inflation pressure was increased.
- The contact pressure patterns obtained for the five-rib tire indicated that higher pressures were obtained for the inner ribs based on the controlled variables for the type of tire evaluated in this study.
- Analytical pavement modeling can be significantly enhanced by using measured tire-pavement contact pressure distribution. With measured tire-pavement contact pressure data, current available pavement analysis programs can more accurately predict actual pavement responses.
- The conventional method that assumes uniform contact stress over a circular area tends to overestimate the pavement responses at high tire pressures.
- Statistical analysis confirmed that pavement responses were significantly related to tire pressure distribution. The ANOVA tests showed that the horizontal strain in the longitudinal direction at the bottom of the asphalt concrete layer and pavement deflections obtained at two different depths are highly sensitive to the pressure distribution.
- Overall, the correct tire contact pressure shape and distribution are needed in order to accurately predict pavement responses. It is recommended to use analytical tools based on more representative material properties (viscoelastic and non-linear properties) to obtain an even better prediction.

References

- Akram, T., Scullion, T., & Smith, R. E. (1993). *Using the multidepth deflectometer to study tire pressure, tire type, and load effects on pavements*. Research report 1184-2 (Vol. 2). College Station, TX: Texas Transportation Institute, Texas A&M University.
- Al-Qadi, I. L., Loulizi, A., Janajreh, I., & Freeman, T. E. (2002). Pavement response to dual tires and new wide-base tires at same tire pressure. *Transportation Research Record*, 1806, 38–47.
- Baker Harris, B., Buth Michael, R., & Van Deusen David, A. (1994). *Minnesota Road research project: Load response instrumentation installation and testing procedures*. Minnesota Department of Transportation.
- Beer, D. et al. (1999). Towards improved mechanistic design of thin asphalt layer surfacing base on actual tire/pavement contact stress-in-motion (SIM) data in South Africa. In *7th conference on asphalt pavements for Southern Africa*, South Africa.
- El-Basyouny, M. M. (2004). *Calibration and validation of asphalt concrete pavements distress models for 2002 design guide*. Ph.D. dissertation, Arizona State University.
- Heavy Vehicle Simulator. (2015). Monitoring of test sections and instrumentation. Retrieved April 2015. <http://www.gautrans-hvs.co.za/>
- Huang, Y. H. (1993). *Pavement analysis and design*. Englewood Cliffs, NJ: Prentice-Hall.
- Leiva-Villacorta, F., Aguiar-Moya, J. P., & Loria-Salazar, L. G. (2013). Ensayos acelerados de pavimento en Costa Rica. *Infraestructura Vial*, 15, 15–19.
- Leiva-Villacorta, F., Aguiar-Moya, J. P., & Loria-Salazar, L. G. (2015). Accelerated pavement testing first results at the Lanammeur APT facility. In *94th annual meeting*. Washington, DC: Transportation Research Board.
- Machemehl, R. B., Wang, F., & Prozzi, J. A. (2005). Analytical study of effects of truck tire pressure on pavements using measured tire-pavement contact stress data. In *CD-ROM proceedings for the 84th TRB annual meeting*. Washington, DC: Transportation Research Board, January 9–13, 2005.
- Mateos, A., & Snyder, M. B. (2002). Validation of flexible pavement structural response models with data from the Minnesota Road Research Project. *Transportation Research Record*, 1806, 19–29.
- NCHRP. (2004a). *Guide for mechanistic-empirical design of new and rehabilitated pavements structures*. Final document, Appendix RR finite element procedures for flexible pavement analysis. Washington, DC: National Cooperative Highway Research Program.
- NCHRP. (2004b). *Guide for mechanistic-empirical design of new and rehabilitated pavements structures*. Final report, part 3 design analysis. Washington, DC: National Cooperative Highway Research Program.
- Prozzi, J. A., & Luo, R. (2005). Quantification of the joint effect of wheel load and tire inflation pressure on pavement response. In *CD-ROM for TRB 2005 annual meeting*. Washington, DC: Transportation Research Board.
- Roque, R., et al. (2000). Evaluating measured of tire contact stresses predict pavement response and performance. *Transportation Research Record*, 1716, 73–81.
- Sebaaly, P. E., & Tabatabaee, N. (1992). Effect of tire parameters on pavement damage and load-equivalency factors. *ASCE Journal of Transportation Engineering*, 118(6), 805–819.
- Sibaja, L. M. (2014). *Determinación de presión de neumáticos de vehículos de carga típicos de Costa Rica*. Costa Rica: Trabajo Final de Graduación, Universidad de Costa Rica.
- Siddharthan, R. V., Krishnamenon, N., El-Mously, M., & Sebaaly, P. E. (2002). Investigation of tire contact stress distributions on pavement response. *ASCE Journal of Transportation Engineering*, 128(2), 136–144.
- Ullidtz, P. (1987). Pavement analysis. In *Development in civil engineering* (Vol. 19). Amsterdam, The Netherlands: Elsevier.

- Wang, F., & Machemehl, R. B. (2006). Mechanistic-empirical study of effects of truck tire pressure on pavement using measured tire-pavement contact stress data. In *85th TRB annual meeting*. Washington, DC: Transportation Research Board.
- Weissman, S. L. (1999). Influence of tire-pavement contact stress distribution on development of distress mechanisms in pavements. *Transportation Research Record*, 1655, 161–167.